Spontaneous self-ordered states of vortex-antivortex pairs in a polariton condensate

F. Manni,[1,*] T. C. H. Liew,[2] K. G. Lagoudakis,[3] C. Ouellet-Plamondon,[1] R. André,[4] V. Savona,[5] and B. Deveaud[1]

[1]*Institute of Condensed Matter Physics, École Polytechnique Fédérale de Lausanne (EPFL), CH-1015 Lausanne, Switzerland*
[2]*Division of Physics and Applied Physics, Nanyang Technological University, 63737 Singapore*
[3]*E. L. Ginzton Laboratory, Stanford University, Stanford, California 93405-4088, USA*
[4]*Institut Néel, CNRS, 25 Avenue des Martyrs, 38042 Grenoble, France*
[5]*Institute of Theoretical Physics, Ecole Polytechnique Fédérale de Lausanne (EPFL), CH-1015 Lausanne, Switzerland*
(Received 14 February 2013; published 15 November 2013)

Polariton condensates have proved to be model systems to investigate topological defects, as they allow for direct and nondestructive imaging of the condensate complex order parameter. The fundamental topological excitations of such systems are quantized vortices. In specific configurations, further ordering can bring the formation of vortex lattices. In this work we demonstrate the spontaneous formation of ordered vortical states, consisting in geometrically self-arranged vortex-antivortex pairs. A mean-field generalized Gross-Pitaevskii model reproduces and supports the physics of the observed phenomenology.

Quantized vortices are fundamental and ubiquitous entities across physics, playing a central role in mechanisms ranging from galaxy formation to phase conformation in microscopic quantum systems. They represent topological excitations of quantum degenerate Bose gases, such as Bose-Einstein condensates (BEC), superfluids, and superconductors.[1] Throughout the past decades, these systems have offered the unprecedented opportunity of studying such topological defects and their phenomenology in a direct and controlled way.[1] Under peculiar conditions, quantized vortices have the unique property of arranging themselves in geometrically ordered structures, such as the Abrikosov lattices.[2,3] Vortex lattices were first observed in type-II superconductors under magnetic fields,[4] then in both superfluids[5] and atom BEC,[6–9] by setting the system into rotation, and also in optical nonlinear systems.[10–12] Ultimately, in the limit of high vortex density, these lattices are predicted to undergo a quantum phase transition to strongly correlated states, similar to quantum Hall states, that still represent an open experimental challenge.[1]

Recently, exciton polaritons have established themselves as a model two-dimensional Bose gas.[13] Such quasiparticles arise as the eigenmodes of the strong-coupling regime between light and matter, which was demonstrated in planar semiconductor microcavities.[14] The polariton system being dissipative in nature, due to the finite lifetime of the quasiparticles, has phenomenology intrinsically and strongly out of equilibrium. Thus, continuous optical pumping is required to replenish the polariton population. Shaping of the excitation conditions allows manipulation of the condensate phenomenology in a simple way, unveiling striking physical effects. Moreover, thanks to the mixed light-matter components of polaritons, the emitted photons inherit all the properties of the quantum fluid that can, thus, be fully characterized by optical measurement of the extracavity field.[15]

After the recent demonstration of polariton condensation[16] and superfluidity[17] in semiconductor microcavities, much effort has been devoted to the study of quantum turbulence and vorticity, under different excitation conditions, in such out-of-equilibrium quantum fluids.[18–20] In particular, quantized vortices were demonstrated to spontaneously occur in the system as topological defects pinned by the disorder potential,[21] which naturally results from the sample growth process. In addition, vortex-antivortex dipoles have been reported,[18,22] in analogy to reports in atomic BEC.[23] Following the striking demonstrations of collective vortex phenomena in atom BEC, a number of proposals and theoretical investigations considered means for the formation of vortex lattices in polariton condensates, both in the scalar[24–27] and spinor condensate case.[25,26] Methods for detecting the rotating lattice have also been proposed for the experimental observation.[28] Recent demonstrations of vortex lattices were provided by engineering the interference of multiple independent condensates,[29] bringing the topic to the forefront of polariton research. Very recently, the spontaneous formation of a vortex lattice under coherent resonant excitation of a polariton parametric oscillator was also reported.[30]

In this Rapid Communication, we demonstrate the spontaneous occurrence of polariton condensed states composed of geometrically self-arranged vortex-antivortex pairs, using nonresonant excitation (equivalent to an incoherent pumping). Each vortex having its counter-rotating partner, the overall state carries no orbital angular momentum. We perform interferometric measurements allowing the determination of the amplitude and the phase of the condensate order parameter, directly imaging the vortical entities. Theoretically, a mean-field approach reproduces the vortex-antivortex lattice formation and identifies the different possible phases of the system, which depend on the pump intensity and its spatial size.

The sample is the same CdTe planar semiconductor microcavity, featuring 26 meV of Rabi splitting, used in our previous experiments.[16,21,31] The sample is kept in a He-cooled cryostat at approximately 4 K. As mentioned, a key feature for the stabilization of vortex-antivortex lattices lies in the careful shaping of the intensity profile of the pump laser.

The principle is to create a ring-shaped intensity profile, similar to a Bessel beam, with a large central spot of the same intensity as the outer ring. The reduced intensity valley between the central spot and the outer ring acts as the guide

for the stabilization of vortex-antivortex pairs. Simply using a Gaussian-shaped pump would not be enough, since vortices are known to be dynamically unstable in such a configuration.[32] The shaping of the beam is done by employing a single conical lens—*axicon*—in combination with two lenses (L1, L2) and a 0.5 N.A. microscope objective (MO), according to the scheme depicted in Fig. 1(a). The initial top-hat laser beam is transformed into a Bessel beam by using the axicon. In the transformation, intermediate intensity profiles are generated, as the one used in this work [Fig. 1(b)], which is then imaged by lenses L1 and L2 in the real space of the sample, through the MO. Fine tuning of the excitation is allowed by a system of relative micrometric positioning between the axicon and the lenses.

We excite the system above condensation threshold with the intensity-shaped pump beam at a power of $\approx 250\ \mu$W. The photoluminescence (PL) coming from the sample is collected by the same MO and is then sent to a modified Mach-Zehnder interferometer, which takes the condensate image and interferes it with a $4\times$ magnified replica of the central spot [marked by the dashed rectangle in Fig. 2(a)]. This allows one to take a small part of the condensate, acting as phase reference, overlap it with the whole condensate image, and extract its phase structure, as performed in Ref. 31. From the interference pattern, the phase can then be extracted by digital off-axis holographic techniques.[33] Despite the presence of a disorder potential,[34] some regions of shallow disorder are present in the CdTe sample that allow the formation of vortex lattices.

To explain the whole process, we first consider a set of data showing a four-vortex lattice, composed of tw vortex-antivortex pairs. The condensate density image [Fig. 2(a)] is interfered with the enlarged version of the central spot of the condensate [Fig. 2(b)]. The resulting pattern is shown

FIG. 2. (Color online) (a) Polariton condensate density at a position where a four-vortex lattice is observed. (b) Magnified central part of the condensate [marked by the dashed rectangle in panel (a)] used to overlap with the full condensate to obtain the interference pattern, shown in (c). The corresponding phase structure is plotted in (d). Red (green) circles mark the position of vortex (antivortex).

in Fig. 2(c) together with the corresponding phase structure reported in Fig. 2(d). In the figure, two vortex-antivortex pairs can easily be identified, marked by the red (vortex, clockwise phase winding) and green (antivortex, counterclockwise phase winding) circles at the position of the phase dislocation. Observing the real space phase map, when circumventing the center of the condensate cloud, one finds alternately vortex/antivortex entities. Let us point out that some spurious phase singularities (with no circular marker on top) appear in a region of negligible density, outside the condensed polariton gas. They are resulting from the overlap of the decaying outer tails of the condensate with the edges of the flat phase reference.

It is possible to create vortex lattices of higher order, where more vortex-antivortex pairs are able to accommodate in the same alternate ordered way. By slightly increasing the size of the pump spot (in the 1 μm range) while keeping its intensity profile as in Fig. 1(b), we could find other positions on the sample where the disorder allowed the formation of the six-vortex lattice. The results are summarized in Fig. 3. The condensate density, featuring six clear density minima is shown in Fig. 3(a). The vortex cores are evidenced also by taking a circular profile of the density,[35] shown in Fig. 3(b). The vertical dashed lines identify the position of six clear relative density minima, vortex cores, along the azimuthal profile. By analysis of the orientation of the forklike dislocations in the interference pattern [Fig. 3(c)] and corresponding phase structure [Fig. 3(d)], one can clearly identify the position of
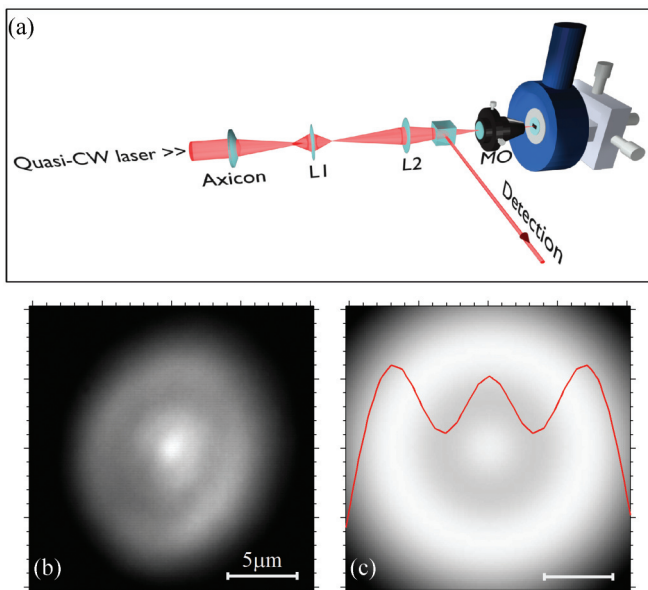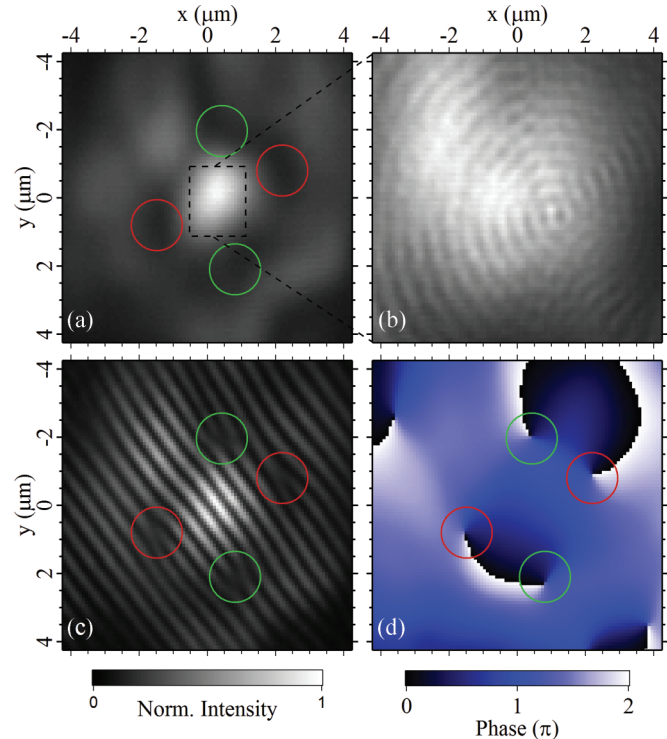

FIG. 1. (Color online) (a) Scheme of the setup used to engineer the excitation. A typical shaped intensity profile is shown in (b), averaged over many disorder realizations. (c) Intensity profile for the pump beam used in the theoretical calculations. The red line depicts the cross-section intensity profile of the beam.
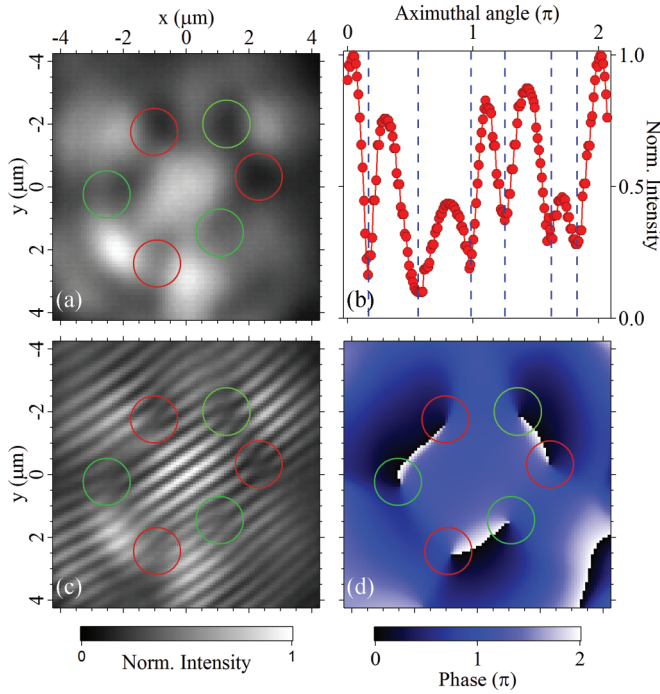
FIG. 3. (Color online) (a) Polariton condensate density at a position where a six-vortex lattice is observed. (b) Profile taken around the central spot of the condensate that highlights the relative minima, identifying the core of the six vortices (each vertical line marks the minimum position). (c) Interference pattern from which the phase structure is extracted, as shown in (d). Red (green) circles mark the position of vortex (antivortex).

the phase dislocations and the winding sign of each vortex. The red and green colored circles, as in the case of Fig. 2, mark the alternating vortex-antivortex lattice. Despite the presence of the underlying disorder potential felt by the polaritons, the six-lattice nicely matches a hexagonal structure. Indeed, the disorder pins the direction of the lattice in real space and accounts for the distortions with respect to an exact symmetric lattice, theoretically expected in absence of any cylindrical symmetry breaking.

Polariton condensation under nonresonant pumping is a highly nonequilibrium process. Being coherent, the condensate itself can be treated with a Gross-Pitaevskii-type equation coupled to a classical rate equation for the dynamics of an exciton reservoir,[36] which appropriately models the incoherent excitations generated by nonresonant pumping that feed and interact with the condensate. Both spectral and spatial features coming from experiments have been successfully reproduced within this theoretical framework[37–40] and also adapted to take into account the dynamic properties of polariton condensates[41–43] and of spinor condensates.[44,45] The equations read

$$i\hbar \frac{\partial \psi(\mathbf{r},t)}{\partial t} = \left\{ \hat{E}_{LP} + V(\mathbf{r}) + \frac{i\hbar}{2}[R_R n(\mathbf{r},t) - \gamma_c] \right\} \psi(\mathbf{r},t),$$

(1)

$$\frac{\partial n(\mathbf{r},t)}{\partial t} = -(\gamma_R + R_R|\psi(\mathbf{r},t)|^2)n(\mathbf{r},t) + P(\mathbf{r}),$$

(2)

where $\psi(\mathbf{r},t)$ is the polariton condensate in the mean-field representation and $n(\mathbf{r},t)$ is the intensity distribution of the incoherent excitonic reservoir, directly injected by the nonresonant pump. For the purpose of this work the polarization degree of freedom of polaritons is neglected. $\hat{E}_{LP}$ is the polariton kinetic energy operator, accounting for the nonparabolicity of the dispersion of lower branch polaritons. $V(\mathbf{r})$ represents an effective potential, given by the mean-field shift induced by polariton-polariton interactions (g), the interaction of polaritons with the reservoir (g_R), and an additional pump-induced shift (G);[36] $V(\mathbf{r}) = \hbar g|\psi(\mathbf{r},t)|^2 + \hbar g_R n(\mathbf{r},t) + \hbar G P(\mathbf{r})$, where g, g_R, and G are constants. $P(\mathbf{r})$ represents the spatial pump distribution, as in Fig. 1(c). The intracondensate interactions between polaritons being present but small, the dominant effects determining the induced effective potential come from the effect of the exciton reservoir on condensed polaritons.[37] γ_c and γ_R represent the decay rates of condensed polaritons and reservoir excitons, respectively. R_R is the stimulated scattering rate of excitons from the reservoir to the condensate and thus represents the condensation rate in the system. The system of two coupled equations (1) and (2) is numerically solved in time. The initial conditions for seeding the condensate consist of an initial random low-intensity white noise. We performed a systematic study of the system under the custom intensity-shaped pump beam of Fig. 1(c), for varying pump ring size and power. The calculations allow drawing a phase diagram, where several different regions, corresponding to species of vortical solutions, are found.[46] In particular, both the experimentally observed lattice configurations are identified as stationary solutions.

Figure 4 shows one of the stationary solutions found in the phase diagram. The intensity and phase of the polariton condensate, calculated with this method,[47] are in good agreement with the experimental findings (Fig. 3). Due to the nonequilibrium nature of our exciton-polariton system, the spatially inhomogeneous pump leads to currents in the steady state that connect the regions of net gain and loss. As pointed out in Ref. 24, these supercurrents can significantly alter condensate density profiles. Furthermore, steady-state current flows in a rotationally symmetric system have been shown to be unstable to breaking of the rotational symmetry and new stationary and localized states can be stabilized by nonlinear losses.[48] Our situation is similar to that of Ref. 24, where a parabolic trap was used to generate spatially inhomogeneous flow. While in high density regions, fluctuations are damped
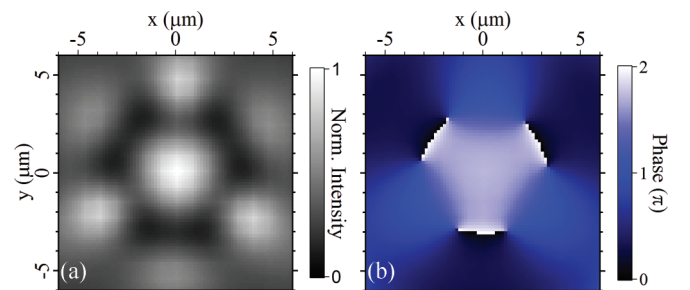

FIG. 4. (Color online) Theoretically calculated polariton condensate density (a) and phase structure (b) that nicely matches the experimental results of Fig. 3.

by nonlinear coupling to the exciton reservoir, fluctuations in low density regions grow. This caused instability into higher angular momentum modes and the spontaneous appearance of vortex lattices. To realize this experimentally, we have used an inhomogeneous pumping to induce an effective trapping of polaritons. From the shape of the pump profile, one can expect a preferential growth of the condensate into a central spot and an outer ring. In the region between them, there is instability into the initially low density angular momentum modes.

Theoretically, the system reaches the same steady vortex lattice pattern independent of the initial noise. The initial noise may, however, affect the time required for formation of the lattice. One can note that the vortex lattice pattern is not cylindrically symmetric (although it has a rotational symmetry of third order). Theoretically, the breaking of cylindrical symmetry could be caused by the initial noise, in which case the pattern would form with a different overall orientation (but otherwise identical shape) from shot to shot. Our system is, however, not perfectly symmetrical to begin with; imperfections in the pump profile and disorder already break the system symmetry allowing the pattern to form with the same orientation from shot to shot and be observed in multishot averaged experiments.[31] While the process of polariton condensation itself represents a spontaneous symmetry breaking, and the formation of patterns in polariton condensates is often considered an example of spontaneous pattern formation,[24,30,49] it should be noted that our configurations do not represent the unstable states that would be associated with a Kosterlitz-Thouless-type phase transition.

Furthermore, it is worth mentioning that the disorder plays an important role in the determination of the energy of the condensate, substantially influencing the potential landscape felt by the particles, so that only at a few specific sample positions could we obtain the engineered pump-induced trapping of the vortices and observe the lattice formation. At such positions, slight adjustment of the pump beam alignment allows fine tuning of the symmetry and stability of the lattice itself.

In this work we have reported on the formation and stabilization of vortex lattices, composed of vortex-antivortex pairs, in a polariton condensate. Ordered patterns are observed under proper intensity-shaped nonresonant optical pumping. The shaping is such to create a trap for vortices that are seen to arrange in a geometrical vortex lattice. A delicate interplay between the excitation shape and the underlying disorder potential pins the orientation of the spatial patterns, allowing their detection in time-integrated experiments. We make use of a mean-field approach in the form of a generalized Gross-Pitaevskii model that is able to reproduce the lattice formation under the same kind of excitation conditions used in the experiments. The control over the lattice formation could prove to be useful in Bose gases when considering the few particle per vortex limit, which is expected to give rise to quantum phase transitions to highly correlated states[1]—a world yet to be explored. Recent long-lifetime polaritons achieved in GaAs cavities[50] represent to this extent really promising systems.

*Present address: Institute for Quantum Electronics, ETH Zürich, CH-8093 Zürich, Switzerland; francesco.manni@epfl.ch

[1] A. L. Fetter, J. Low Temp. Phys. **161**, 445 (2010).

[2] A. A. Abrikosov, Sov. Phys. JETP **5**, 1174 (1957).

[3] A. A. Abrikosov, Rev. Mod. Phys. **76**, 975 (2004).

[4] U. Essmann and H. Träuble, Phys. Lett. A **24**, 526 (1967).

[5] E. J. Yarmchuk, M. J. V. Gordon, and R. E. Packard, Phys. Rev. Lett. **43**, 214 (1979).

[6] M. R. Matthews, B. P. Anderson, P. C. Haljan, D. S. Hall, C. E. Wieman, and E. A. Cornell, Phys. Rev. Lett. **83**, 2498 (1999).

[7] K. W. Madison, F. Chevy, W. Wohlleben, and J. Dalibard, Phys. Rev. Lett. **84**, 806 (2000).

[8] J. R. Abo-Shaeer, C. Raman, J. M. Vogels, and W. Ketterle, Science **292**, 476 (2001).

[9] V. Schweikhard, I. Coddington, P. Engels, S. Tung, and E. A. Cornell, Phys. Rev. Lett. **93**, 210403 (2004).

[10] G. A. Swartzlander and C. T. Law, Phys. Rev. Lett. **69**, 2503 (1992).

[11] J. Scheuer and M. Orenstein, Science **285**, 230 (1999).

[12] J. W. Fleischer, M. Segev, N. K. Efremidis, and D. N. Christodoulides, Nature (London) **422**, 147 (2003).

[13] I. Carusotto and C. Ciuti, Rev. Mod. Phys. **85**, 299 (2013).

[14] C. Weisbuch, M. Nishioka, A. Ishikawa, and Y. Arakawa, Phys. Rev. Lett. **69**, 3314 (1992).

[15] V. Savona and F. Tassone, Solid State Commun. **95**, 673 (1995).

[16] J. Kasprzak, M. Richard, S. Kundermann, A. Baas, P. Jeambrun, J. M. J. Keeling, F. M. Marchetti, M. H. Szymanska, R. Andre, J. L. Staehli *et al.*, Nature (London) **443**, 409 (2006).

[17] A. Amo, D. Sanvitto, F. P. Laussy, D. Ballarini, E. del Valle, M. D. Martin, A. Lemaitre, J. Bloch, D. N. Krizhanovskii, M. S. Skolnick *et al.*, Nature (London) **457**, 291 (2009).

[18] D. N. Krizhanovskii, D. M. Whittaker, R. A. Bradley, K. Guda, D. Sarkar, D. Sanvitto, L. Vina, E. Cerda, P. Santos, K. Biermann *et al.*, Phys. Rev. Lett. **104**, 126402 (2010).

[19] G. Grosso, G. Nardin, F. Morier-Genoud, Y. Léger, and B. Deveaud-Plédran, Phys. Rev. Lett. **107**, 245301 (2011).

[20] D. Sanvitto, F. M. Marchetti, M. H. Szymanska, G. Tosi, M. Baudisch, F. P. Laussy, D. N. Krizhanovskii, M. S. Skolnick, L. Marrucci, A. Lemaitre *et al.*, Nat. Phys. **6**, 527 (2010).

[21] K. G. Lagoudakis, M. Wouters, M. Richard, A. Baas, I. Carusotto, R. Andre, L. S. Dang, and B. Deveaud-Plédran, Nat. Phys. **4**, 706 (2008).

[22] G. Roumpos, M. D. Fraser, A. Loffler, S. Hofling, A. Forchel, and Y. Yamamoto, Nat. Phys. **7**, 129 (2011).

[23] T. W. Neely, E. C. Samson, A. S. Bradley, M. J. Davis, and B. P. Anderson, Phys. Rev. Lett. **104**, 160401 (2010).

[24] J. Keeling and N. G. Berloff, Phys. Rev. Lett. **100**, 250401 (2008).

[25] T. C. H. Liew, Y. G. Rubo, and A. V. Kavokin, Phys. Rev. Lett. **101**, 187401 (2008).

[26] J. Keeling and N. G. Berloff, arXiv:1102.5302v2 (2011).

[27] A. V. Gorbach, R. Hartley, and D. V. Skryabin, Phys. Rev. Lett. **104**, 213903 (2010).

[28] M. O. Borgh, G. Franchetti, J. Keeling, and N. G. Berloff, Phys. Rev. B **86**, 035307 (2012).

[29] G. Tosi, G. Christmann, N. G. Berloff, P. Tsotsis, T. Gao, Z. Hatzopoulos, P. G. Savvidis, and J. J. Baumberg, Nat. Commun. **3**, 1243 (2012).

[30] K. Guda, M. Sich, D. Sarkar, P. M. Walker, M. Durska, R. A. Bradley, D. M. Whittaker, M. S. Skolnick, E. A. Cerda-Méndez, P. V. Santos *et al.*, Phys. Rev. B **87**, 081309 (2013).

[31] F. Manni, K. G. Lagoudakis, T. C. H. Liew, R. André, and B. Deveaud-Plédran, Phys. Rev. Lett. **107**, 106401 (2011).

[32] E. A. Ostrovskaya, J. Abdullaev, A. S. Desyatnikov, M. D. Fraser, and Y. S. Kivshar, Phys. Rev. A **86**, 013636 (2012).

[33] K. G. Lagoudakis, T. Ostatnicky, A. V. Kavokin, Y. G. Rubo, R. Andre, and B. Deveaud-Plédran, Science **326**, 974 (2009).

[34] D. N. Krizhanovskii, K. G. Lagoudakis, M. Wouters, B. Pietka, R. A. Bradley, K. Guda, D. M. Whittaker, M. S. Skolnick, B. Deveaud-Plédran, M. Richard *et al.*, Phys. Rev. B **80**, 045317 (2009).

[35] The circular profile is obtained from the interference pattern, from which both the the condensate density and phase are extracted.

[36] M. Wouters, I. Carusotto, and C. Ciuti, Phys. Rev. B **77**, 115340 (2008).

[37] G. Roumpos, W. H. Nitsche, S. Hofling, A. Forchel, and Y. Yamamoto, Phys. Rev. Lett. **104**, 126403 (2010).

[38] M. Wouters, T. C. H. Liew, and V. Savona, Phys. Rev. B **82**, 245315 (2010).

[39] G. Christmann, G. Tosi, N. G. Berloff, P. Tsotsis, P. S. Eldridge, Z. Hatzopoulos, P. G. Savvidis, and J. J. Baumberg, Phys. Rev. B **85**, 235303 (2012).

[40] P. Cristofolini, A. Dreismann, G. Christmann, G. Franchetti, N. G. Berloff, P. Tsotsis, Z. Hatzopoulos, P. G. Savvidis, and J. J. Baumberg, Phys. Rev. Lett. **110**, 186403 (2013).

[41] G. Nardin, K. G. Lagoudakis, M. Wouters, M. Richard, A. Baas, R. André, L. S. Dang, B. Pietka, and B. Deveaud-Plédran, Phys. Rev. Lett. **103**, 256402 (2009).

[42] K. G. Lagoudakis, B. Pietka, M. Wouters, R. André, and B. Deveaud-Plédran, Phys. Rev. Lett. **105**, 120403 (2010).

[43] K. G. Lagoudakis, F. Manni, B. Pietka, M. Wouters, T. C. H. Liew, V. Savona, A. V. Kavokin, R. André, and B. Deveaud-Plédran, Phys. Rev. Lett. **106**, 115301 (2011).

[44] F. Manni, K. G. Lagoudakis, T. C. H. Liew, R. André, V. Savona, and B. Deveaud, Nat. Commun. **3**, 1309 (2012).

[45] E. Kammann, T. C. H. Liew, H. Ohadi, P. Cilibrizzi, P. Tsotsis, Z. Hatzopoulos, P. G. Savvidis, A. V. Kavokin, and P. G. Lagoudakis, Phys. Rev. Lett. **109**, 036404 (2012).

[46] See Supplemental Material at http://link.aps.org/supplemental/10.1103/PhysRevB.88.201303 for the calculated phase diagram and a detailed discussion.

[47] We used the following parameters in the simulations: $\hbar\gamma_c = 1$ meV, $\hbar\gamma_R = 10$ meV, $\hbar R_R = 0.1$ meV μm^2, $G = 0.01$ μm^2, and $\hbar g_R = 0.033$ meV μm^2.

[48] M. A. Porras, A. Parola, D. Faccio, A. Dubietis, and P. Di Trapani, Phys. Rev. Lett. **93**, 153902 (2004).

[49] F. M. Marchetti, M. H. Szymańska, C. Tejedor, and D. M. Whittaker, Phys. Rev. Lett. **105**, 063902 (2010).

[50] B. Nelsen, G. Liu, M. Steger, D. W. Snoke, R. Balili, K. West, and L. Pfeiffer, arXiv:1209.4573v2 [Phys. Rev. X (to be published)].